Research Article | Vol. 26, No. 20 | 1 Oct 2018 | OPTICS EXPRESS 25944
Optics EXPRESS

Deterministic coupling of quantum emitters in WSe_2 monolayers to plasmonic nanocavities

OLIVER IFF,[1] NILS LUNDT,[1] SIMON BETZOLD,[1] LAXMI NARAYAN TRIPATHI,[1,2] MONIKA EMMERLING,[1] SEFAATTIN TONGAY,[3] YOUNG JIN LEE,[4] SOON-HONG KWON,[4] SVEN HÖFLING,[1,5] AND CHRISTIAN SCHNEIDER[1,*]

[1]*Technische Physik and Wilhelm Conrad Röntgen Research Center for Complex Material Systems, Physikalisches Institut, Universität Würzburg, Am Hubland, D-97074 Würzburg, Germany*
[2]*Present Address: Department of Physics, Birla Institute of Technology, Mesra, Ranchi 835215, Jharkhand, India*
[3]*School for Engineering for Matter, Transport, and Energy, Arizona State University, Tempe, Arizona 85287, USA*
[4]*Department of Physics, Chung-Ang University, Seoul, South Korea*
[5]*SUPA, School of Physics and Astronomy, University of St. Andrews, St. Andrews, KY16 9SS, UK*
[*]*christian.schneider@physik.uni-wuerzburg.de*

Abstract: We discuss coupling of site-selectively induced quantum emitters in exfoliated monolayers of WSe_2 to plasmonic nanostructures. Gold nanorods of 20 nm-240 nm size, which are arranged in pitches of a few micrometers on a dielectric surface, act as seeds for the formation of quantum emitters in the atomically thin materials. We observe characteristic narrow-band emission signals from the monolayers, which correspond well with the positions of the metallic nanopillars with and without thin dielectric coating. Single photon emission from the emitters is confirmed by autocorrelation measurements, yielding $g^2(\tau = 0)$ values as low as 0.17. Moreover, we observe a strong co-polarization of our single photon emitters with the frequency matched plasmonic resonances, as a consequence of light-matter coupling. Our work represents a significant step towards the scalable implementation of coupled quantum emitter-resonator systems for highly integrated quantum photonic and plasmonic applications.

1. Introduction

Engineering solid state quantum emitters and their integration in micro- and nanophotonic structures is one of the prime tasks in modern quantum engineering. Coupled solid state quantum emitter-cavity systems range among the most promising candidates for the realization of highly efficient single photon sources [1–5], spin photon interfaces [6,7], quantum sensing probes [8] as well as building blocks for quantum simulation [9] and surface code quantum computing [10]. While quantum emitters have been identified, studied and engineered in a variety of crystals including III-V [11] and II-VI quantum dots [12–14], color defects in diamonds [15], impurities in SiC and organic polymers [16,17], atomically thin materials [18–22] were recently established as a novel platform of quantum photonic devices. Quantum dots in III-V semiconductors [23] and defect centers in diamonds [24] certainly belong to the most mature implementations, but the quality of site-controlled emitters still needs to be improved, putting a serious thread regarding their scalable fabrication in ordered arrays. Ordered InAs/GaAs quantum dot arrays have been realized by selective area growth methods and epitaxial growth on patterned substrates [26], but in most cases the costly fabrication methods severely compromised their emission properties. Direct integration of positioned solid state quantum emitters with photonic resonators has been accomplished [27–29], but only in few selected cases, and genuine scalability has remained elusive.

#334805 https://doi.org/10.1364/OE.26.025944
Journal © 2018 Received 11 Jun 2018; revised 8 Aug 2018; accepted 14 Aug 2018; published 20 Sep 2018

Optics EXPRESS

The formation of quantum emitters in mono- and bilayers of transition metal dichalcogenides has now been studied in various implementations: initially, localized luminescence centers in exfoliated flakes were discovered close to their edges, and have been associated with strain wrinkles [20–22]. In epitaxially grown flakes, random positioning of such spots was observed [18], indicating emission from defect bound excitons. Recently, the formation of quantum emitters on modulated metal substrates [30, 31], as well as nanopillars [32, 33] was reported and associated with localized and engineered crystal strain fields, which outlines the unique possibility to deterministically induce quantum emitters in a straight forward manner by structuring the sample surface prior to the transfer of the monolayer.

While the ordered formation of quantum emitters thus far has been mainly observed on dielectric, nanostructured surfaces, spontaneous emission enhancement was reported on rough metallic surfaces and gold-coated nanopillars, giving rise to localized plasmonic modes [31]. Combining atomically thin materials which comprise either tightly localized excitons or strongly bound free excitons with nanoplasmonic cavities yields a promising pathway to study light-matter coupling on the nanoscale enabled by the enormous field enhancements provided by metallic nanostructures [34–38].

2. Sample structure and setup

In this work, we demonstrate the feasibility to induce ordered arrays of quantum emitters by defined arrays of metallic nanopillars, fabricated on a SiO_2 substrate. Such structures directly represent a coupled quantum dot-nanocavity system, and act as polarization-controlled single photon sources.

The sample consists of a semi-insulating silicon substrate, with a 200 nm thick SiO_2 layer on top. In order to fabricate the nanopillars, we first spin-coated a thin layer of PMMA and performed electron beam lithography to selectively expose rectangular areas in the resist with dimensions of 20 nm - 240 nm. After developing the resist, a 80 nm thick gold layer was evaporated on the sample, followed by a lift-off step. A scanning electron microscope (SEM) image of a prototype nanopillar array with a pitch of 2 µm is shown in Fig. 1(a). On selected samples we additionally deposited a 5 nm thin layer of Al_2O_3 via atomic layer deposition. Next, we fabricated atomically thin layers of WSe_2 via mechanical exfoliation using adhesive tape, and transferred the layers on the pillar arrays via dry transfer [39] (Fig. 1(b)). We observe, that part of the pillars pierced the monolayer, while a substantial number of nanopillars (> 50 %) locally strained the layer, yielding the tent-like structure shown in Fig. 1(c).

Spatially resolved optical spectroscopy was performed in a micro-photoluminescence (μPL) setup with a high spatial resolution (≈ 0.5 µm using fiber based confocal setting). The sample is excited by a frequency-doubled Nd:YAG laser at 532 nm, mounted in a liquid helium cooled flow cryostat. A direct comparison of the PL of different pillars with and without Al_2O_3 is presented in Fig. 1(d), which shows no significant quenching or change in intensity in the absence of the thin oxide layer.

3. Experimental results and discussion

Figure 2(a) depicts an exemplaric series of power dependent luminescence spectra recorded on the position of a nanopillar with dielectric coating. The spectrum is widely dominated by a zoo of sharp emission lines, a typical signature of strongly localized emission centers in the crystal. In Fig. 2(b) we plot the excitation power (P_{exc}) dependent PL intensity I of such an emitter, while fitting it with the simple two-level approximation $I = I_{sat}/(1 + P_n/P_{exc})$. Here, I_{sat} is the saturation intensity and P_n is a free fit parameter to normalize the power. The observed saturation at moderate pump powers is a signature of an intrinsic blocking mechanism, provided by the finite lifetime of a localized two-level system.

Optics EXPRESS

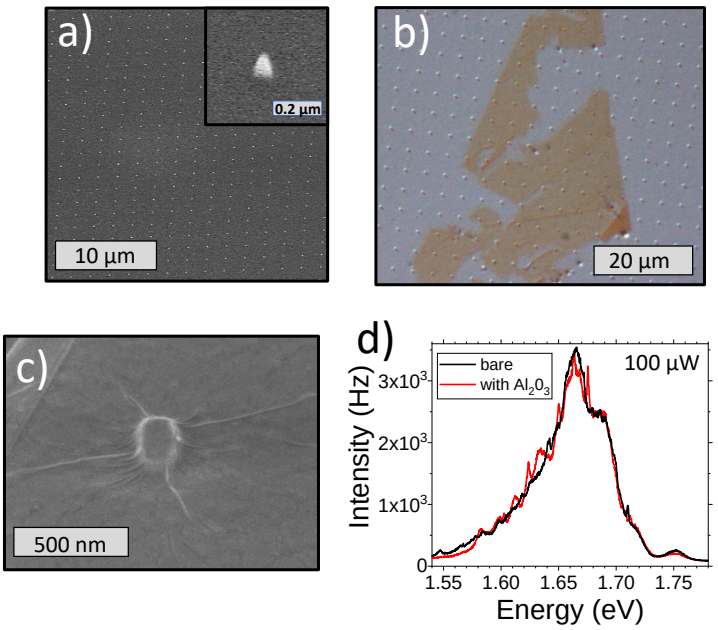

Fig. 1. a) Scanning electron microscope (SEM) image of the sample surface comprising metallic nanopillars as quantum emitter seeds and plasmonic nano-cavities. Inset: close-up view of a nanopillar. b) Optical image of the pillar array after successful dry-transfer of an atomically thin WSe_2 monolayer. c) Close-up SEM image of a single pillar covered by a strained monolayer, showing the formation of wrinkles. d) Comparison of the photoluminescence of pillars covered by WSe_2 with and without Al_2O_3 coating at 100 µW. No significant influence or quenching is observed.

The ordered formation of emitters on the nanopillar arrays is confirmed in a highly spatially resolved scanning (μPL) study, applying the confocal configuration: Here, we carefully scan the sample's surface by utilizing a pair of motorized linear stages with a step width of 500 nm underneath the excitation and collection spot. The spectrally integrated map (700 nm-800 nm) is shown in Fig. 2(c). It clearly evidences a regular pattern of bright emission sites, perfectly coinciding with the positions of the metallic pillars with a pitch of 4 µm (dashed black pattern). Spectral information is best illustrated in a selected linescan between the blue arrows in Fig. 2(c). Here, we clearly observe a two-fold effect by the nanopillars (Fig. 2(d)): A strong luminescence enhancement of up to 100% occuring at the positions of the nano-pillars compared to off-pillar, signifies a resonant optical coupling to a plasmonic resonance [40], as well as the regular formation of the sharp peaks below the free exciton energy (<1.74 eV), which we associate with tight exciton localization due to strain.

In order to provide evidence for the capability to emit single photons from the deterministically localized excitons, we performed second order correlation measurements by exciting the sample with a 532 nm CW laser (Fig. 3(a)). We selected a dominant emission feature from one square pillar (140 nm × 140 nm). The luminescence was spectrally filtered (selected bandwidth: ≈ 1 meV, 300 grooves/mm grating) and passed to a fiber coupled Hanbury Brown and Twiss (HBT) setup. We observed a well-pronounced anti-bunching signal at zero delay time ($\tau = 0$), allowing us to extract a $g^{(2)}(\tau = 0)$ value of 0.17 ± 0.15, which clearly puts our system in the regime of single photon emission.

Polarization resolved spectroscopy on different nanopillars revealed a strongly linear polar-

Optics EXPRESS

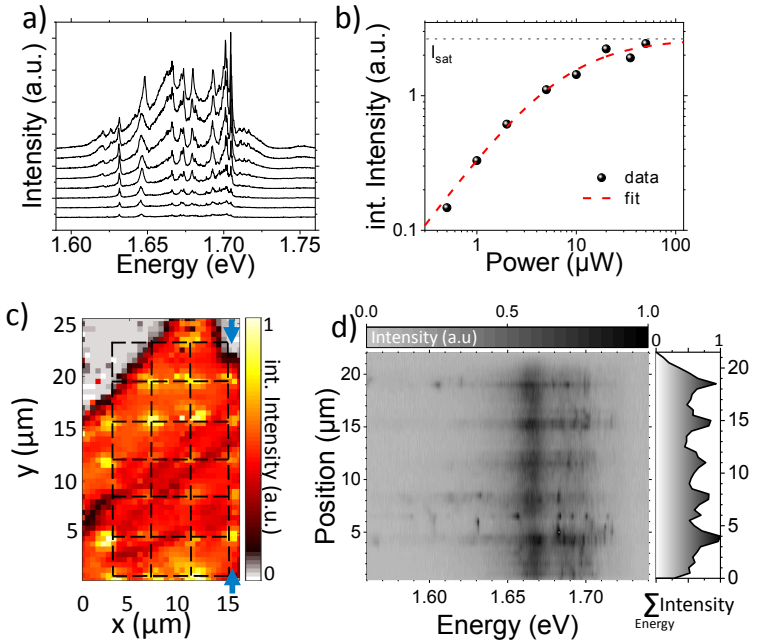

Fig. 2. a) Power-dependent spectra on a nanopillar revealing many discrete emitters. b) Power-dependent study of a quantum emitter emission line before saturation starts above 10 μW. c) Spatial map of a WSe_2 flake covering the nano-pillar array, showing the integrated intensity from 700 – 800 nm. The enhanced PL coincides with the 4 μm pillar distance (black pattern). d) Spectral information extracted between the blue arrows in c), revealing a periodic increase in luminescence and the formation of additional localized emission centers at the pillar positions.

ization of the luminescence from the emitters. In Fig. 3(b) two exemplary 90 nm × 30 nm pillars are shown which are aligned perpendicular to each other and covered by the same monolayer. Comparing the polarization of several emitters from these two pillars shows a strong correspondence of the polarization and pillar orientation (Figs. 3(c) and (d)). This alignment of the polarization along the long axis of the gold rectangle can be associated with the coupling of the emitter to the plasmonic excitations in the metal which are much more pronounced in the extended axes as has been demonstrated with similar plasmonic structures before [41]. Slight modification of the rotation angle also depends on the way the monolayer bends around the pillar, which further acts on the polarization of the emission [42].

4. Simulation

In order to understand the optical enhancement of the quantum emitters in a WSe_2 via a metal nanopillar, we investigated the plasmon modes excited by finite-difference time-domain (FDTD) method. Two geometries have been considered: a rod-like nanopillar and a square pillar as experimentally studied above. In the square pillar with a size of 140 nm × 140 nm, the electric field distribution on top surface of the pillar is calculated, as shown in Fig. 4(a), where a quantum emitter of WSe_2 can be placed. At two vertical side edges orthogonal to the E_x polarization, strong field enhancement (E/E_0) with a maximum value of 20 compared with an incident light is observed. In addition, the vector plot shows, that the field enhancement is strongly attributed from the E_x field at the edges. Because the emitter in 2D materials oscillates in plane, strong emission enhancement for the defect emitters at the edges can be induced by the resonant coupling

Optics EXPRESS

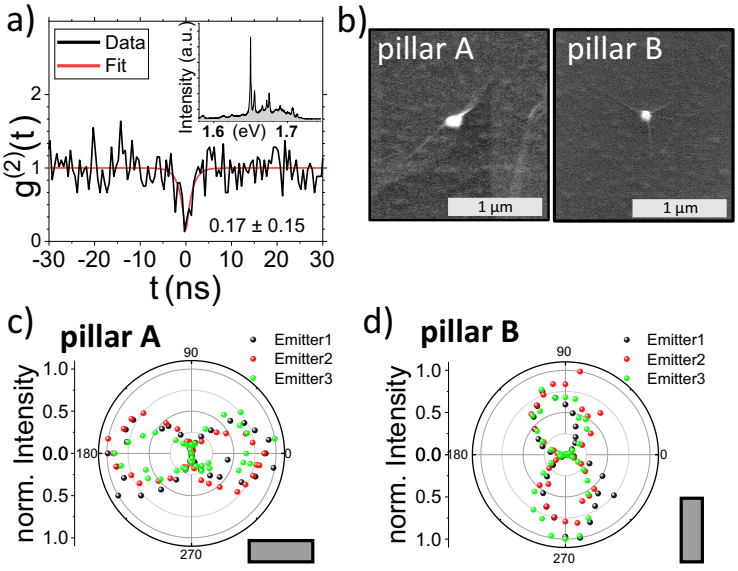

Fig. 3. a) Second-order autocorrelation function of a quantum emitter on a pillar. The value of $g^{(2)}(\tau = 0) = 0.17 \pm 0.15$ confirms single photon emission. Inset: spectrum of single photon emitter. b) SEM images of two individual rectangles covered by WSe_2. Pillar A is horizontally and pillar B vertically aligned. c) and d) Polarization characteristic of three individual quantum emitters each on two different 90 nm × 30 nm nanopillars shown in b).

of the plasmon mode. The mode of Fig. 4(a) is obtained by assuming E_x linearly polarized incident light, and a 90-degree rotated mode (not shown in the Fig.) can also be observed for E_y polarized incident light. The scattering cross-section spectra, which are plotted in Fig. 4(b), visualize the spectral dependence of the plasmonic mode in a square pillar for different sizes of the side edges from 40 nm to 140 nm, where the resonant peak for a size of 140 nm × 140 nm is centered around 733 nm with a large FWHM of 234 nm. Therefore, the radiative emission of the quantum emitter with a spectrum of Fig. 2(a) can be enhanced by resonant coupling with a plasmonic mode. As expected, the plasmon resonance shifts blue with decreasing the size.

In order to understand the strong polarization dependence of the emission from a rod-like nanopillar as shown in Figs. 3(c) and (d), the mode profile and the scattering cross-section of such a nanopillar with the experimentally studied cross-section of 90 nm × 30 nm are investigated. For the E_x polarized incident light, the electric field distribution of the plasmonic mode in Fig. 4(c) resembles that of our square pillar, Fig. 4(a) except for that the mode is elongated along the x-direction following the rod-like shape. In the scattering cross-section spectrum, the rod-like pillar exhibits strong plasmon resonance peak at a wavelength of 686 nm for an E_x polarized light, however, there are no significant resonances for an E_y polarized light (Fig. 4(d)). Therefore, 90 nm × 30 nm nanopillar can enhance the x-directionally polarized emission of a quantum emitter and selectively suppress the y-directionally polarized emission, resulting in strong linear polarization aligned along the long axis, as shown in Figs. 3(c) and (d).

5. Summary

In conclusion, we demonstrated the formation of ordered arrays of quantum emitters in an atomically thin layer of WSe_2, transferred on a metal nanorod array. The metallic nanostructures yield the formation of quantum emitters, and furthermore can act as plasmonic resonators granting active polarization control via deterministic light-matter coupling. Our work is a first

Optics EXPRESS

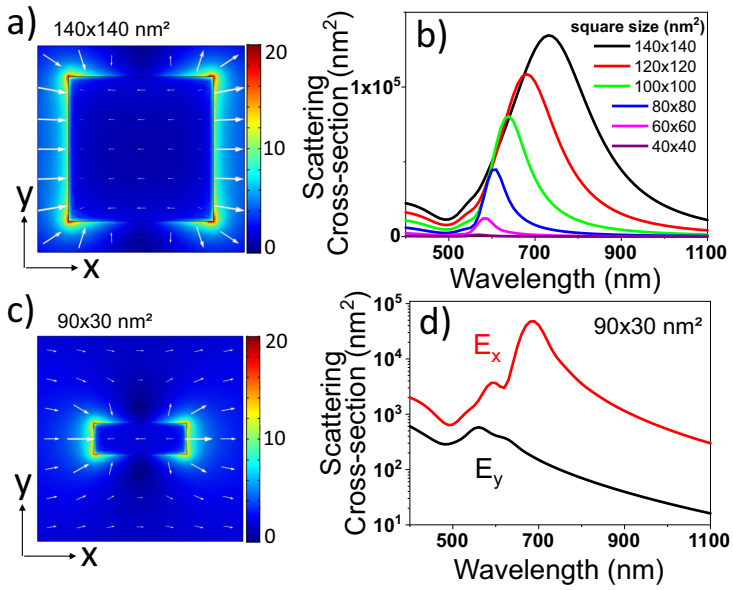

Fig. 4. FDTD simulation: Vector maps of the field distribution and electric field enhancement E/E_0 at top surface of a pillar with a) a square cross-section of (140 nm × 140 nm) and c) a rod-like cross-section of (90 nm × 30 nm) excited by an electromagnetic field E_0 of 1 V/m at 740 nm. b) Calculated scattering cross-section spectrum of square nanopillars with different size from 140 nm to 40 nm. d) Two scattering cross-section spectrums of a rod-like nanopillar with a size of 90 nm × 30 nm for an incident light with orthogonal polarizations, E_x (red) and E_y (black). X-direction represents the direction of the long edge of the rod-like nanopillar.

step towards highly scalable cavity quantum electrodynamics with engineered quantum emitters in two dimensional materials.

During the preparation of this report, we became aware of two similar studies claiming light-matter coupling with ordered quantum emitters on plasmonic nanostructures [43, 44].

Funding

State of Bavaria, European Research Council [with the project unLiMIt2D (679228)]; National Research Foundation of Korea, Korean Government Grant (NRF-2016R1C1B2007007); National Science Foundation (DMR-1552220[, DMR-1838443]).

References

1. X. Ding, Y. He, Z. C. Duan, N. Gregersen, M. C. Chen, S. Unsleber, S. Maier, C. Schneider, M. Kamp, S. Höfling, C. Y. Lu, and J. W. Pan, "On-Demand Single Photons with High Extraction Efficiency and Near-Unity Indistinguishability from a Resonantly Driven Quantum Dot in a Micropillar," Phys. Rev. Lett. **116**, 1–6 (2016).
2. A. Schlehahn, A. Thoma, P. Munnelly, M. Kamp, S. Höfling, T. Heindel, C. Schneider, and S. Reitzenstein, "An electrically driven cavity-enhanced source of indistinguishable photons with 61% overall efficiency," APL Photonics **1**, 011301 (2016).
3. S. Unsleber, Y.-M. He, S. Maier, S. Gerhardt, C.-Y. Lu, J.-W. Pan, M. Kamp, C. Schneider, and S. Höfling, "Highly indistinguishable on-demand resonance fluorescence photons from a deterministic quantum dot micropillar device with 74 % extraction efficiency," Opt. Express **24**, 1023–1030 (2015).
4. P. Senellart, G. Solomon, and A. White, "High-performance semiconductor quantum-dot single-photon sources," Nat. Nanotechnol. **12**, 1026–1039 (2017).
5. W. H. Chang, W. Y. Chen, H. S. Chang, T. P. Hsieh, J. I. Chyi, and T. M. Hsu, "Efficient single-photon sources based on low-density quantum dots in photonic-crystal nanocavities," Phys. Rev. Lett. **96**, 3–6 (2006).

Optics EXPRESS

6. K. De Greve, L. Yu, P. L. McMahon, J. S. Pelc, C. M. Natarajan, N. Y. Kim, E. Abe, S. Maier, C. Schneider, M. Kamp, S. Höfling, R. H. Hadfield, A. Forchel, M. M. Fejer, and Y. Yamamoto, "Quantum-dot spin-photon entanglement via frequency downconversion to telecom wavelength," Nature **491**, 421–425 (2012).
7. W. B. Gao, P. Fallahi, E. Togan, J. Miguel-Sanchez, and A. Imamoğlu, "Observation of entanglement between a quantum dot spin and a single photon," Nature **491**, 426–430 (2012).
8. J. N. Anker, W. P. Hall, O. Lyandres, N. C. Shah, J. Zhao, and R. P. Van Duyne, "Biosensing with plasmonic nanosensors," Nat. Mater. **7**, 442–453 (2008).
9. H. Wang, Y. He, Y.-H. Li, Z.-E. Su, B. Li, H.-L. Huang, X. Ding, M.-C. Chen, C. Liu, J. Qin, J.-P. Li, Y.-M. He, C. Schneider, M. Kamp, C.-Z. Peng, S. Höfling, C.-Y. Lu, and J.-W. Pan, "High-efficiency multiphoton boson sampling," Nat. Photonics **11**, 361 (2017).
10. K. D. Greve, D. Press, P. L. McMahon, and Y. Yamamoto, "Ultrafast optical control of individual quantum dot spin qubits," Reports on Prog. Phys. **76** (2013).
11. P. Michler, A. Imamoğlu, M. D. Mason, P. J. Carson, G. F. Strouse, and S. K. Buratto, "Quantum correlation among photons from a single quantum dot at room temperature," Nature **406**, 968–970 (2000).
12. X. Peng, L. Manna, W. Yang, J. Wickham, E. Scher, A. Kadavanich, and A. P. Alivisatos, "Shape control of CdSe nanocrystals," Nature **404**, 59–61 (2000).
13. M. Lowisch, M. Rabe, B. Stegemann, F. Henneberger, M. Grundmann, V. Türck, and D. Bimberg, "Zero-dimensional excitons in (Zn,Cd)Se quantum structures." Phys. review. B, Condens. matter **54**, R11074 (1996).
14. S. H. Xin, P. D. Wang, A. Yin, C. Kim, M. Dobrowolska, J. L. Merz, and J. K. Furdyna, "Formation of self-assembling CdSe quantum dots on ZnSe by molecular beam epitaxy," Appl. Phys. Lett. **69**, 3884–3886 (1996).
15. C. Kurtsiefer, S. Mayer, P. Zarda, and H. Weinfurter, "Stable solid-state source of single photons," Phys. Rev. Lett. **85**, 290–293 (2000).
16. S. Castelletto, B. C. Johnson, V. Ivády, N. Stavrias, T. Umeda, A. Gali, and T. Ohshima, "HL 113 : Quantum information systems II (with TT)," Nat. Mater. **12**, 1–6 (2013).
17. S. Castelletto, B. C. Johnson, C. Zachreson, D. Beke, I. Balogh, T. Ohshima, I. Aharonovich, and A. Gali, "Room temperature quantum emission from cubic silicon carbide nanoparticles," ACS Nano **8**, 7938–7947 (2014).
18. Y.-M. He, G. Clark, J. R. Schaibley, Y. He, M.-C. Chen, Y.-J. Wei, X. Ding, Q. Zhang, W. Yao, X. Xu, C.-Y. Lu, and J.-W. Pan, "Single quantum emitters in monolayer semiconductors," Nat. Nanotechnol. **10**, 497–502 (2015).
19. A. Srivastava, M. Sidler, A. V. Allain, D. S. Lembke, A. Kis, and A. Imamoglu, "Optically active quantum dots in monolayer WSe2," Nat. Nanotechnol. **10**, 491–496 (2015).
20. P. Tonndorf, R. Schmidt, R. Schneider, J. Kern, M. Buscema, G. a. Steele, A. Castellanos-Gomez, H. S. J. van der Zant, S. Michaelis de Vasconcellos, and R. Bratschitsch, "Single-photon emission from localized excitons in an atomically thin semiconductor," Optica **2**, 347 (2015).
21. M. Koperski, K. Nogajewski, A. Arora, V. Cherkez, P. Mallet, J.-Y. Veuillen, J. Marcus, P. Kossacki, and M. Potemski, "Single photon emitters in exfoliated WSe2 structures," Nat. Nanotechnol. **10**, 503–506 (2015).
22. S. Kumar, A. Kaczmarczyk, and B. D. Gerardot, "Strain-Induced Spatial and Spectral Isolation of Quantum Emitters in Mono- and Bilayer WSe2," Nano Lett. **15**, 7567–7573 (2015).
23. Y. He, X. Ding, Z. E. Su, H. L. Huang, J. Qin, C. Wang, S. Unsleber, C. Chen, H. Wang, Y. M. He, and X. L. Wang, "Time-bin-encoded boson sampling with a single-photon device," Phys. Rev. Lett. **118**(19), 190501 (2017).
24. G. Balasubramanian, I. Y. Chan, R. Kolesov, M. Al-Hmoud, J. Tisler, C. Shin, C. Kim, A. Wojcik, P. R. Hemmer, A. Krueger, T. Hanke, A. Leitenstorfer, R. Bratschitsch, F. Jelezko, and J. Wrachtrup, "Nanoscale imaging magnetometry with diamond spins under ambient conditions," Nature **455**, 648–651 (2008).
25. T. Van Der Sar, E. C. Heeres, G. M. Dmochowski, G. De Lange, L. Robledo, T. H. Oosterkamp, and R. Hanson, "Nanopositioning of a diamond nanocrystal containing a single nitrogen-vacancy defect center," Appl. Phys. Lett. **94**, 92–95 (2009).
26. O. G. Schmidt, *Lateral alignment of epitaxial quantum dots* (Springer Science & Business Media, 2007).
27. P. Gallo, M. Felici, B. Dwir, K. Atlasov, K. F. Karlsson, A. Rudra, A. Mohan, G. Biasiol, L. Sorba, and E. Kapon, "Integration of site-controlled pyramidal quantum dots and photonic crystal membrane cavities," Appl. Phys. Lett. **263101**, 1–4 (2008).
28. C. Schneider, T. Heindel, A. Huggenberger, P. Weinmann, C. Kistner, M. Kamp, S. Reitzenstein, S. Höfling, and A. Forchel, "Single photon emission from a site-controlled quantum dot-micropillar cavity system," Appl. Phys. Lett. **94**, 1–4 (2009).
29. T. Sünner, C. Schneider, M. Strauss, A. Huggenberger, D. Wiener, S. Höfling, M. Kamp, and A. Forchel, "Scalable fabrication of optical resonators with embedded site-controlled quantum dots." Opt. letters **33**, 1759–1761 (2008).
30. J. Kern, I. Niehues, P. Tonndorf, R. Schmidt, D. Wigger, R. Schneider, T. Stiehm, S. Michaelis de Vasconcellos, D. E. Reiter, T. Kuhn, and R. Bratschitsch, "Nanoscale Positioning of Single-Photon Emitters in Atomically Thin WSe2," Adv. Mater. pp. 7101–7105 (2016).
31. L. N. Tripathi, O. Iff, S. Betzold, M. Emmerling, K. Moon, Y. J. Lee, S.-H. Kwon, S. Höfling, and C. Schneider, "Spontaneous emission enhancement in strain-induced WSe2 monolayer based quantum light sources on metallic surfaces," ACS Photonics **5**, 1919–1926 (2018).
32. C. Palacios-Berraquero, D. M. Kara, A. R. Montblanch, M. Barbone, P. Latawiec, D. Yoon, A. K. Ott, M. Loncar, A. C. Ferrari, and M. Atatüre, "Large-scale quantum-emitter arrays in atomically thin semiconductors," Nat. Commun. **8**, 1–6 (2017).

Optics EXPRESS

33. A. Branny, S. Kumar, R. Proux, and B. D. Gerardot, "Deterministic strain-induced arrays of quantum emitters in a two-dimensional semiconductor," Nat. Commun. **8**, 1–7 (2017).
34. A. Krasnok, S. Lepeshov, and A. Alú, "Nanophotonics with 2D Transition Metal Dichalcogenides," ArXiv **1801.00698** (2018).
35. P. Lalanne, W. Yan, K. Vynck, C. Sauvan, and J.-P. Hugonin, "Light Interaction with Photonic and Plasmonic Resonances," Laser & Photonics Rev. **1700113**, 1700113 (2018).
36. T. T. Tran, D. Wang, Z. Q. Xu, A. Yang, M. Toth, T. W. Odom, and I. Aharonovich, "Deterministic Coupling of Quantum Emitters in 2D Materials to Plasmonic Nanocavity Arrays," Nano Lett. **17**, 2634–2639 (2017).
37. J. Chaste, A. Missaoui, S. Huang, H. Henck, Z. Ben Aziza, L. Ferlazzo, C. Naylor, A. Balan, A. T. Johnson, R. Braive, and A. Ouerghi, "Intrinsic Properties of Suspended MoS2on SiO2/Si Pillar Arrays for Nanomechanics and Optics," ACS Nano **12**, 3235–3242 (2018).
38. B. Mukherjee, N. Kaushik, R. P. N. Tripathi, A. M. Joseph, P. K. Mohapatra, S. Dhar, B. P. Singh, G. V. P. Kumar, E. Simsek, and S. Lodha, "Exciton Emission Intensity Modulation of Monolayer MoS2 via Au Plasmon Coupling," Sci. Reports **7**, 41175 (2017).
39. A. Castellanos-Gomez, M. Buscema, R. Molenaar, V. Singh, L. Janssen, H. S. J. van der Zant, and G. a. Steele, "Deterministic transfer of two-dimensional materials by all-dry viscoelastic stamping," 2D Mater. **1**, 011002 (2014).
40. J. T. Hugall, A. Singh, and N. F. Van Hulst, "Plasmonic Cavity Coupling," ACS Photonics **5**, 43–53 (2018).
41. Y. Luo, E. D. Ahmadi, K. Shayan, Y. Ma, K. S. Mistry, C. Zhang, J. Hone, J. L. Blackburn, and S. Strauf, "Purcell-enhanced quantum yield from carbon nanotube excitons coupled to plasmonic nanocavities," Nat. Commun. **8** (2017).
42. J. Kern, A. Trügler, I. Niehues, J. Ewering, R. Schmidt, R. Schneider, S. Najmaei, A. George, J. Zhang, J. Lou, U. Hohenester, S. Michaelis De Vasconcellos, and R. Bratschitsch, "Nanoantenna-Enhanced Light-Matter Interaction in Atomically Thin WS2," ACS Photonics **2**, 1260–1265 (2015).
43. Y. Luo, G. D. Shepard, J. V. Ardelean, J. C. Hone, and S. Strauf, "Deterministic coupling of site-controlled quantum emitters in monolayer semiconductors to plasmonic nanocavities." arXiv Mesoscale Nanoscale Phys. **1050**, 1804.06541 (2018).
44. T. Cai, J.-h. Kim, Z. Yang, S. Dutta, S. Aghaeimeibodi, and E. Waks, "Radiative enhancement of single quantum emitters in WSe2 monolayers using site-controlled metallic nano-pillars," arXiv p. 1803.09358 (2018).